*Computers, Materials & Continua* CMC, vol.60, no.2, pp.757-765, 2019

# Ab Initio Molecular-Dynamics Simulation Liquid and Amorphous $Al_{94-x}Ni_6La_x$ (x=3-9) Alloys

**Lu Wang[1, 2], Cuihhong Yang[2], Tong Liu[3] and Hongyan Wu[2, *]**

**Abstract:** Ab initio molecular-dynamics simulations have been used to investigate the liquid and amorphous $Al_{94-x}Ni_6La_x$ (x=3-9) alloys. Through calculating the pair distribution functions and partial coordination numbers, the structure and properties of these alloys are researched, which will help the design bulk metallic glass. The concentration of La atoms can affect the short-range order of $Al_{94-x}Ni_6La_x$ alloys, which is also studied in this calculation result.

**Keywords:** Molecular dynamics simulation, liquid and amorphous alloys, pair distribution functions.

## 1 Introduction

Amorphous and nanocrystalline Al-TM-RE alloys (TM=transition metal, RE=rare-earth elements) have gained an increasing attention due to their promising mechanical properties, and especially their high strength combined with good ductility, which are superior to those of conventional high-strength Al-alloys [Inoue (1998); He, Poon and Shiflet (1988)]. Numerous studies have been carried out on the properties, structure and glass formation ability (GFA) of Al-Ni-RE alloys [Kawamura, Inoue and Masumoto (1993); Li, Gu, Xie et al. (2013); Yang, Wang and Li (2008); Kim, Inoue and Masumoto (1990)]. Among the known Al-based alloys, Al-Ni-La alloy is one of the most potential systems to directly form bulk metallic glass [Kim, Inoue and Masumoto (1991); Li, Wang, Bian et al. (2010)]. Sanders et al reported that a maximum glass-forming composition was $Al_{86}La_5Ni_9$ in the Al-La-Ni system and the maximum amorphous thickness was 780 mm [Sanders, Warner and Miracle (2006)]. On the other hand, the crystallization of amorphous Al-Ni-La alloys more depends on the La content than Al-Ni-Y (Y=Ce, Sm, Gd) alloys [Sahoo, Wollgarten, Haug et al. (2005)]. It is important to research the GFA of Al-Ni alloys with the addition of La. The content of La can also effects the properties of alloys after quenching. However, to our knowledge, the dependence of the concentration of the structural of liquid and amorphous Al-Ni-La alloys has not been studied from the first principles yet. It is obvious that an ab initio

[1] Jiangsu Key Laboratory for Optoelectronic Detection of Atmosphere and Ocean, Nanjing University of Information Science & Technology, Nanjing, 210044, China.

[2] Department of Physics, School of Physics & Optoelectronic Engineering, Nanjing University of Information Science & Technology, Nanjing, 210044, China.

[3] School of Physics and Astronomy, Queen Mary University of London, London E1 4NS, UK.

[*] Corresponding Author: Hongyan Wu. Email: wuhongyan12345@163.com.

investigation of the properties of these systems might provide valuable information to clarify the experimental results. Therefore, this paper intends to explore the capabilities of the DFT approach in the generalized gradient approximation (GGA) to provide a realistic picture of various liquid and amorphous $Al_{94-x}Ni_6La_x$ (x=3-9) alloys.

## 2 Computational methods

Our MD calculations have been performed at 2000K by using the Vienna ab initio simulation program VASP [Kresse and Furthmller (1996)] with the projector augmented wave (PAW) method [Blöchl (1994); Kresse and Joubert (1999)]. The calculations presented here are based on density functional theory within the generalized gradient approximation (GGA). Our GGA calculations use the PW91 function due to Perdew et al. [Perdew and Wang (1992)]. We have considered seven concentrations of $Al_{94-x}Ni_6La_x$ (x=3-9). In each case, we used a cubic 100-atom supercell with periodic boundary conditions. The atomic densities for the seven concentrations were obtained from the measured density of $Al_{86}La_5Ni_9$ at this temperature [Sanders, Warner and Miracle (2006)], together with Vegard Law. We use 460eV cutoff for the energies of the plane waves, and $\Gamma$ -point sampling for the supercell Brillouin zone. For the electronic structure, we used Fermi-surface broadening corresponding to an electronic subsystem temperature of $k_BT$=0.1eV. In calculating the electronic wave functions, at each concentration where we include ten empty bands. We control the ionic temperature by using the Nosé-Hoover thermostat [Nosé (1984); Hoover (1985)]. The equations-of-motion are integrated by means of the Verlet algorithm, using an ionic time step of 3fs. The initial atomic configuration is a random distribution of 100 atoms on the grid for each concentration. Then, the system is heated up to 2000K by rescaling the ionic velocities. After equilibration for 4ps at this temperature, we reduce the temperature to 400K with the cooling rate of $1.5\times10^{12}$ K/s. The physical quantities of interest were obtained by averaging over 10ps after the initial equilibration taking 3ps.

## 3 Results and discussion

### *3.1 Liquid $Al_{94-x}Ni_6La_x$ alloys*

The atom-atom and total pair distribution functions of liquid $Al_{94-x}Ni_6La_x$ (x=3-9) alloys are calculated at 2000K. The Al-Al pair distribution functions are depicted in Fig. 1(a). The first peak of $g_{Al\text{-}Al}(r)$ becomes higher from 2.37 for x=3 to 2.60 for x=9 with increasing La concentration. Here it also can be appreciated that the Al-Al atoms induce a larger degree of short-range order. Given the partial pair distribution functions, it is possible to calculate the partial coordination numbers as

$$N_{\alpha\beta} = 2\int_0^{R_{\max}} 4\pi r^2 \rho_\beta g_{\alpha\beta(r)} dr$$

where $R_{max}$ is the first maximum coordinate (the nearest-neighbor distanced) in $g_{\alpha\beta}$. The calculated nearest-neighbor distances and the partial coordination number of Al-Al are listed in Tab. 1. The value of the average Al-Al bond length is about 2.67Å which is a little smaller than the sum of two single aluminum atomic radius (2.86Å). It shows that there is the interaction between Al atoms. On the other hand, the partial coordination number $N_{Al\text{-}Al}$

decreases from 10.74 for x=3 to 9.77 for x=9 with increasing La atoms. It is because that the La atom replaced the Al atom and the atomic number of aluminum decreased.

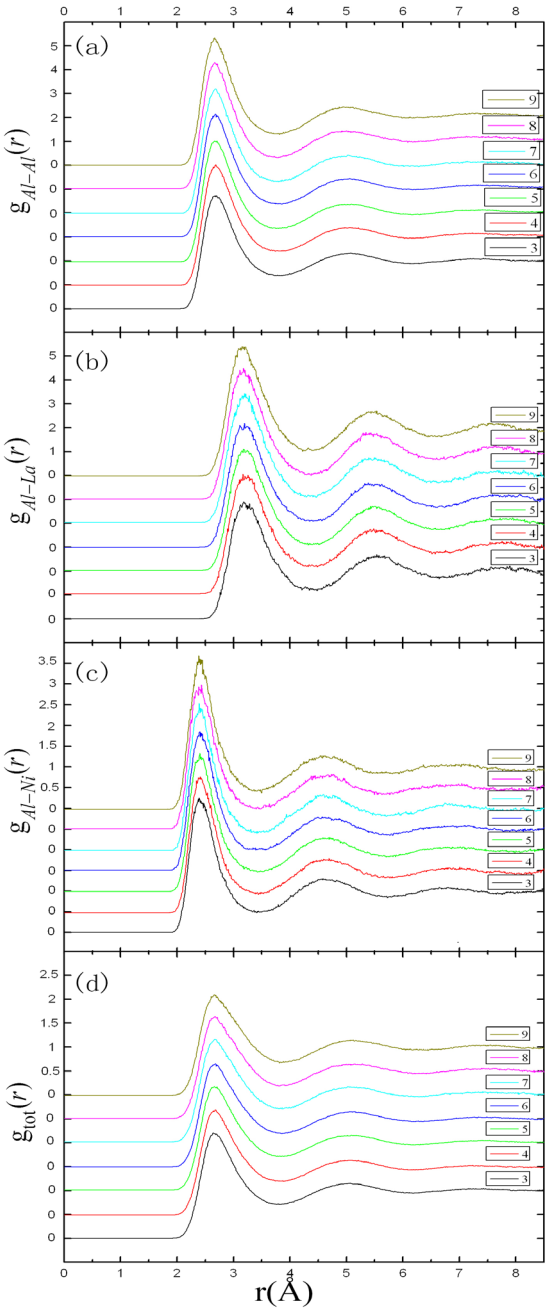


**Figure 1:** The pair distribution functions of liquid $Al_{94-x}Ni_6La_x$ (x=3-9) alloys. Figs. 1(a)-1(c) show the Al-Al, Al-La and Al-Ni pair distribution functions. Fig. 1(d) shows the total pair distribution functions

Compared with the pair distribution functions $g_{Al-Al}(r)$, the position of the first peak of $g_{Al-La}(r)$ moves right clearly in Fig. 1(b). It is because that the radius of La atom (1.83 Å) is larger than the radius of Al atom (1.43Å). The value of the average Al-La bond length is about 3.19Å (see Tab. 1) which is very close to the sum of Al atomic radius and La atomic radius (3.26Å). It shows that the interaction between Al atoms and La atoms was weak. The first peak of $g_{Al-La}(r)$ becomes higher from 2.45 for x=3 to 2.71 for x=9 with increasing La concentration. It shows that the short-range order of alloys was increased. As a small number of La atoms, the partial coordination number $N_{Al-La}$ is small in Tab. 1. It also shows that the distribution of La atoms did not form the cluster.

**Table 1:** The calculated nearest-neighbor distance r (Å) and coordination number N for liquid $Al_{94-x}Ni_6La_x$ alloys

| x | Al-Al | | Al-La | | Al-Ni | | total | |
|---|---|---|---|---|---|---|---|---|
| | r | N | r | N | r | N | r | N |
| 3 | 2.68 | 10.74 | 3.19 | 0.57 | 2.40 | 0.57 | 2.65 | 11.79 |
| 4 | 2.68 | 10.29 | 3.18 | 0.76 | 2.41 | 0.57 | 2.66 | 11.80 |
| 5 | 2.67 | 10.21 | 3.18 | 0.89 | 2.41 | 0.57 | 2.67 | 11.98 |
| 6 | 2.67 | 10.20 | 3.20 | 1.11 | 2.41 | 0.57 | 2.67 | 12.08 |
| 7 | 2.67 | 10.17 | 3.20 | 1.34 | 2.42 | 0.57 | 2.68 | 12.22 |
| 8 | 2.67 | 9.92 | 3.19 | 1.47 | 2.43 | 0.59 | 2.68 | 12.33 |
| 9 | 2.67 | 9.77 | 3.18 | 1.68 | 2.41 | 0.58 | 2.67 | 12.42 |

Fig. 1(c) exhibits the Al-Ni pair distribution functions. Compared with Figs. 1(a) and 1(b), the position of the first peak of $g_{Al-Ni}(r)$ moves left clearly. The average Al-Ni bond length is 2.41Å (see Tab. 1). It is much less than the sum of Al atomic radius and Ni atomic radius (2.75Å). The first peak height of $g_{Al-Ni}(r)$ is larger than the first peak height of $g_{Al-Al}(r)$ and $g_{Al-La}(r)$, which means the interaction between Al atoms and Ni atoms is the strongest in the interaction of Al, La and Ni atoms. As the number of Ni atoms is constant in the liquid $Al_{94-x}Ni_6La_x$ (x=3-9) alloys, the partial coordination number $N_{Al-Ni}$ is about 0.57.

In Fig. 1(d), the total pair distribution functions of liquid $Al_{94-x}Ni_6La_x$ (x=3-9) alloys are shown. All figures have the diffused and smooth first peak. But the second peak is not obvious in Fig. 1(d). This is the typical characteristics of liquid. As the temperature is high, the position and height of the first peak has hardly any change in all figures of Fig. 1(d). The coordination number increases slightly from 11.79 for x=3 to 12.42 for x=9 in Tab. 1. It is in accord with 11.5 which is the coordination number of liquid pure aluminum.

The mean squared displacement (MSD) is given by

$$MSD=\langle (x(t)-x_0)^2 \rangle$$

where x(t) is the position of the particle at some given time, $x_0$ is the tagged particle's initial position. Fig. 2 shows the mean squared displacement of $Al_{94-x}Ni_6La_x$ (x=4,6,9) alloys at 2000K. The values of MSD all increase as time goes on. It means that those alloys are liquid and have strong liquidity. Our computing result accords with the report

of Gu et al. [Gu, Qin and Bian (2007)]. The slope decreased with the increase of x in Fig. 2. It means the diffusion constant (D) decreases according to the formula

$$D = \lim_{t\to\infty} \frac{1}{6t} < \left| \mathrm{X}_{(t)} - x_0 \right|^2 >$$

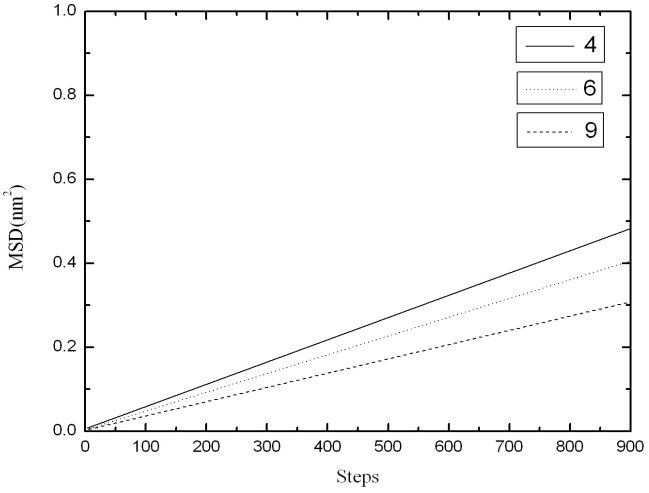


**Figure 2:** The mean squared displacement of $Al_{94-x}Ni_6La_x$ (x=4,6,9) alloys at 2000 K

It can be understood as La atoms are larger than Al and Ni atoms. La atoms check the motion of other atoms with increasing the quantity of La atoms. It causes the decrease of the diffusion constant.

### *3.2 Amorphous $Al_{94-x}Ni_6La_x$ alloys*

The quench simulation of $Al_{94-x}Ni_6La_x$ (x=3-9) alloys are studied in Fig. 3. Those alloys are different from liquid $Al_{94-x}Ni_6La_x$ alloys and all the present properties of amorphous alloys. Fig. 3(a) shows the Al-Al pair distribution functions. Compared with the liquid alloys, the position of the first peak moves right and the height of the first peak becomes larger after quenching. It shows that the degree of short-range order becomes larger in amorphous $Al_{94-x}Ni_6La_x$ alloys than in liquid $Al_{94-x}Ni_6La_x$ alloys. As the large interaction between Al atoms, the second peak appears split. Because Al atoms are replaced by La atoms, the partial coordination number of Al-Al decreases with increasing La concentration (see Tab. 2).

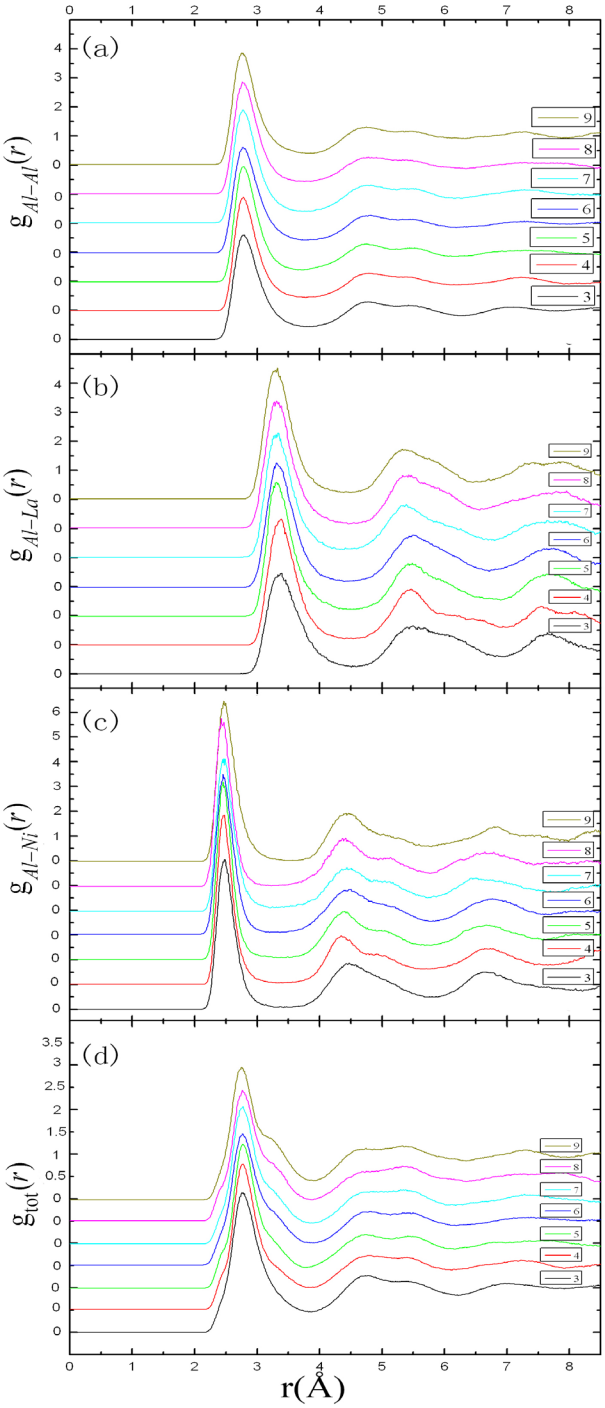


**Figure 3:** The pair distribution functions of amorphous $Al_{94-x}Ni_6La_x$ (x=3-9) alloys. Figs. 3(a)-3(c) show the Al-Al, Al-La and Al-Ni pair distribution functions. Fig. 3(d) shows the total pair distribution functions

In Fig. 3(b), the first peak positions of seven alloys are all beyond 3.32Å which is larger than the sum of Al and La atomic radius (3.26Å). It shows that there is almost not the interaction between Al and La atoms. The first peak becomes sharper with the increasing amount of La atoms, which means the short-range order is enhanced. The second peak is split and the third peak is obvious in Fig. 3(b), which shows these atoms are inclined to the short-range order after quenching. The partial coordination number of Al-La increases with increasing La concentration. Compared with the liquid alloys, the number of the partial coordination number has increased.

The Al-Ni pair distribution functions are depicted in Fig. 3(c). Compared with Fig. 1(c), the location of the first peak has little change. It can be considered that the Al and Ni atoms bound closely together in the amorphous $Al_{94-x}Ni_6La_x$ alloys. The first peak becomes sharp and the second and third peak appears. All these show that the order increases. As the number of Ni atoms does not change in the amorphous $Al_{94-x}Ni_6La_x$ alloys, the partial coordination numbers $N_{Al-Ni}$ are all about 0.56 which is very close to the partial coordination number $N_{Al-Ni}$ of liquid $Al_{94-x}Ni_6La_x$ alloys.

**Table 2:** The calculated nearest-neighbor distance r (Å) and coordination number N for amorphous $Al_{94-x}Ni_6La_x$ alloys

| x | Al-Al | | Al-La | | Al-Ni | | total | |
|---|---|---|---|---|---|---|---|---|
| | r | N | r | N | r | N | r | N |
| 3 | 2.77 | 11.00 | 3.40 | 0.58 | 2.49 | 0.57 | 2.78 | 12.09 |
| 4 | 2.77 | 10.63 | 3.39 | 0.81 | 2.48 | 0.56 | 2.78 | 11.99 |
| 5 | 2.78 | 10.23 | 3.34 | 1.03 | 2.46 | 0.56 | 2.77 | 11.88 |
| 6 | 2.77 | 10.46 | 3.34 | 1.15 | 2.46 | 0.56 | 2.77 | 12.62 |
| 7 | 2.78 | 10.11 | 3.33 | 1.35 | 2.46 | 0.56 | 2.77 | 12.62 |
| 8 | 2.78 | 10.08 | 3.32 | 1.55 | 2.43 | 0.54 | 2.76 | 12.56 |
| 9 | 2.78 | 10.05 | 3.32 | 1.81 | 2.43 | 0.53 | 2.76 | 12.80 |

The total pair distribution functions of amorphous $Al_{94-x}Ni_6La_x$ (x=3-9) alloys are described in Fig. 3(d). As the short-range order increases, the position of the first peak moves right and all peaks become sharp. The second peak is split, which indicates that all compounds are amorphous alloys after quenching. From Tab. 2, the coordination number is about 12 which is in accord with the coordination number of solid pure aluminum and a little larger than liquid aluminum. The computed result is in keeping with the experiment results [Sahoo, Wollgarten, Haug et al. (2005); Roy, Sahoo and Chattoraj (2007); Wollgarten, Sahoo, Hang et al. (2007)].

## 4 Conclusions

In order to improve the glass forming ability of Al-Ni-La alloys, an ab initio investigation has been performed. To understand the nature and mechanism of glass formation, and acquire valuable information for composition design with high GFA, it is of great significance to characterize the atomic structure of liquid and amorphous alloys, and the

structural evolution during the glass transition. The liquid and amorphous $Al_{94-x}Ni_6La_x$ alloys at seven compositions x=3-9 are researched by ab initio molecular-dynamics simulations. These liquid alloys can increase the short-range order and form the amorphous alloys after quenching. Through analyzing the pair distribution functions, it can be found that the interaction between Al and Ni atoms is very strong. However, the interaction between Al and La atoms is almost non-existent. The increase of La atoms makes slow the motion of all atoms, which results in the diffusion constant decreasing.

**Acknowledgement:** This work was supported by the National Natural Science Foundation of China under Grant Nos. 11547030, 11704195. This work was also supported by the Natural Science Foundation-Outstanding Youth Foundation of Jiangsu Province of China (No. BK20160091), and the Six Talent Peaks Project of Jiangsu Province of China (No. GDZB-046).

**References**

**Blöchl, P. E.** (1994): Projector augmented-wave method. *Physical Review B*, vol. 50, no. 24, pp. 17953-17979.

**Gu, T. K.; Qin, J. Y.; Bian, X. F.** (2007): Correlation between local structure of melts and glass forming ability for Al-based alloys: a first-principles study. *Applied Physics Letters*, vol. 91, no. 8, 081907.

**He, Y.; Poon, S. J.; Shiflet, G. J.** (1988): Synthesis and properties of metallic glasses that contain aluminum. *Science*, vol. 241, no. 4873, pp. 1640-1642.

**Hoover, W. G.** (1985): Canonical dynamics: equilibrium phase-space distributions. *Physical Review A*, vol. 31, no. 3, pp. 1695.

**Inoue, A.** (1998): Amorphous, nanoquasicrystalline and nanocrystalline alloys in Al-based systems. *Progress in Materials Science*, vol. 43, no. 1, pp. 365.

**Kawamura, Y.; Inoue, A.; Masumoto, T.** (1993): Mechanical properties of amorphous alloy compacts prepared by a closed processing system. *Scripta Metallurgica et Materialia*, vol. 29, no. 1, pp. 25-30.

**Kim, Y. H.; Inoue, A.; Masumoto, T.** (1990): Ultrahigh tensile strengths of $Al_{88}Y_2Ni_9M_1$ (M=Mn or Fe) amorphous alloys containing finely dispersed FCC-Al particles. *Materials Transactions*, vol. 31, no. 8, pp. 747.

**Kim, Y. H.; Inoue, A.; Masumoto, T.** (1991): Increase in mechanical strength of Al-Y-Ni amorphous alloys by dispersion of nanoscale FCC-Al particles. *Materials Transactions*, vol. 32, no. 4, pp. 331.

**Kresse, G.; Furthmller, J.** (1996): Efficiency of ab-initio total energy calculations for metals and semiconductors using a plane-wave basis set. *Computational Materials Science*, vol. 6, no. 1, pp. 15-50.

**Kresse, G.; Joubert, D.** (1999): From ultrasoft pseudopotentials to the projector augmented-wave method. *Physical Review B*, vol. 59, no. 3, pp. 1758.

**Li, G. H.; Wang, W. M.; Bian, X. F.; Zhang, J. T.; Li, R. et al.** (2010): Influences of similar elements on glass forming ability and magnetic properties in Al-Ni-La amorphous alloy. *Journal of Materials Science & Technology*, vol. 26, no. 2, pp. 146-150.

**Li, Q. F.; Gu, B.; Xie, A. G.; Lian, Y. Y.** (2013): Pressure-induced half-metallicity in $Co_2MnGe_{0.75}Ga_{0.25}$. *Journal of Magnetism and Magnetic Materials*, vol. 346, pp. 192-195.

**Nosé, S.** (1984): A unified formulation of the constant temperature molecular dynamics methods. *Journal of Chemical Physics*, vol. 81, no. 1, pp. 511.

**Perdew, J. P.; Wang, Y.** (1992): Accurate and simple analytic representation of the electron-gas correlation energy. *Physical Review B*, vol. 45, no. 23, pp. 13244.

**Roy, A.; Sahoo, K. L.; Chattoraj, I.** (2007): Electrochemical response of AlNiLa amorphous and devitrified alloys. *Corrosion Science*, vol. 49, no. 6, pp. 2486-2496.

**Sahoo, K. L.; Wollgarten, M.; Haug, J.; Banhart, J.** (2005): Effect of La on the crystallization behavior of amorphous $Al_{94-x}Ni_6La_x$ (x=4-7) alloys. *Acta Materialia*, vol. 53, no. 14, pp. 3861-3870.

**Sanders, W. S.; Warner, J. S.; Miracle, D. B.** (2006): Stability of Al-rich glasses in the Al-La-Ni system. *Intermetallics*, vol. 14, no. 3, pp. 348-351.

**Wollgarten, M.; Sahoo, K. L.; Haug, J.; Banhart, J.** (2007): Influence of La on the crystallisation behaviour of amorphous $Al_{94-x}Ni_6La_x$ (x=4-7) alloys. *Materials Science and Engineering: A*, vol. 449-451, pp. 1049-1051.

**Yang, H.; Wang, J. Q.; Li, Y.** (2008): Influence of TM and RE elements on glass formation of the ternary AL-TM-RE systems. *Journal of Non-Crystalline Solids*, vol. 354, no. 29, pp. 3473-3479.